Tetrahedron xxx (2014) 1–7

Contents lists available at ScienceDirect

Tetrahedron

journal homepage: www.elsevier.com/locate/tet

Sulfur makes the difference: synthesis and mesomorphic properties of novel thioether-functionalized imidazolium ionic liquid crystals

Markus Mansueto, Katharina Christina Kreß, Sabine Laschat *

Institut für Organische Chemie, Universität Stuttgart, Pfaffenwaldring 55, D-70569 Stuttgart, Germany

ARTICLE INFO

Article history:
Received 27 January 2014
Received in revised form 3 March 2014
Accepted 14 March 2014
Available online xxx

Keywords:
Ionic liquid crystals
Sulfur compounds

ABSTRACT

Novel thioether-linked imidazolium ionic liquid crystals were synthesized starting from methyl 2-mercaptoacetate. The mesomorphic properties were determined by differential scanning calorimetry (DSC), polarizing optical microscopy (POM), and X-ray diffraction. All mesogens displayed smectic A mesophase geometries with strongly interdigitated bilayer structures. Comparison of the thioether-linked imidazolium salts with the corresponding amine- and amide-linked imidazolium salts as well as simple *N*-alkyl-imidazolium salts showed that both mesophase width and stability increased with increasing softness of the linking unit, thus indicating the beneficial effect of sulfur. Additionally, an increase of the length of the linking unit decreased the interdigitation of the alkyl chains.

1. Introduction

The introduction of sulfur atoms into organic structures generates a plethora of opportunities regarding molecular electronics applications. Archetypal examples for such sulfur compounds are thiophenes[1] and tetrathiafulvalenes.[2] The incorporation of such moieties in thermotropic liquid crystals is also well known.[3,4] For example, because of the soft character of the sulfur atom due to the more delocalized *d*-orbitals, discotic hexathioalkyltriphenylenes show a decreased electronic band-gap and charge carrier mobilities, which are up to three orders of magnitude larger than those for the corresponding hexaalkoxytriphenylenes.[5,6] The combination of properties of liquid crystals with those of ionic liquids creates the special features of ionic liquid crystals as anisotropically-ordered liquid electrolytes.[7] Very recently, this novel class of materials has been successfully applied as anisotropic lithium ion conductors,[8] as electrolytes in solid-state dye-sensitized solar cells (DSSCs)[9] and in particular, iodine-free DSSCs.[10] Among the various cationic headgroups employed for ionic liquid crystals, imidazolium salts are the most widely used class of compounds.[7d,11] Although some thiophene-based ILCs are known in the literature,[12] the issue of sulfur-containing ILCs is much less explored as compared to classical thermotropic liquid crystals. Based on our recent work on glycine-derived imidazolium ILCs,[13] we noticed that the incorporation of an amine or amide moiety in the side chain influenced mesophase widths significantly as compared to the corresponding *N*-methyl-*N*-alkylimidazolium salts. Thus, we wondered how the replacement of a hard amine by a soft sulfur would affect the mesomorphic properties of ILCs. The results are discussed below.

2. Results and discussion

The synthesis of thioether-containing ILCs **6(C$_n$)X** commenced with the S-alkylation of methyl 2-mercaptoacetate **1** in the presence of K_2CO_3 according to the procedure by Townsend (Scheme 1).[14] Subsequent saponification of the methylester **2** with LiOH in EtOH provided the free carboxylic acid **3**, which was reduced with borane dimethylsulfide to the corresponding alcohol **4**. Compound **4** was submitted to Appel reaction following the procedure by Kukovinets[15] and the resulting bromide **5** was subsequently reacted with *N*-methylimidazole under microwave conditions to give the desired imidazolium bromide **6(C$_n$)Br**. A final salt metathesis step yielded the ILCs **6(C$_n$)X** with different anions.

Mesomorphic properties of thioether-imidazolium ILCs **6(C$_n$)X** were initially studied by differential scanning calorimetry (DSC). The results in Table 1 and Fig. 1 clearly reveal the strong dependence of the mesophase stability on the chain lengths and on the hard/soft character of the counterions. While imidazolium bromide **6(C$_8$)Br** showed no crystallisation point or glass transition in the cooling cycles, a liquid crystalline phase was observed between 22 °C and 51 °C during the heating cycles (Fig. 1a). The corresponding homologous imidazolium bromide **6(C$_{10}$)Br** displayed enantiotropic mesomorphism between 35 °C and 148 °C in the heating cycle and a significant hysteresis possibly due to supercooling (Fig. 1b). However, for compounds **6(C$_n$)Br** with n=12, 14, 16 and 18 the clearing points were shifted to around 200 °C and isotropization was accompanied by decomposition (Table 1 entries 3–6) (Fig. 1c).

Further evidence for the thermal instability of the bromides was verified using thermogravimetric analysis (TGA) (see Supplementary. data, Fig. S1). In prior work we were able to improve the thermal stability by replacing bromide by triflate counterions.[13,16]

* Corresponding author. E-mail address: sabine.laschat@oc.uni-stuttgart.de (S. Laschat).

0040-4020/$ – see front matter © 2014 Elsevier Ltd. All rights reserved.
http://dx.doi.org/10.1016/j.tet.2014.03.050

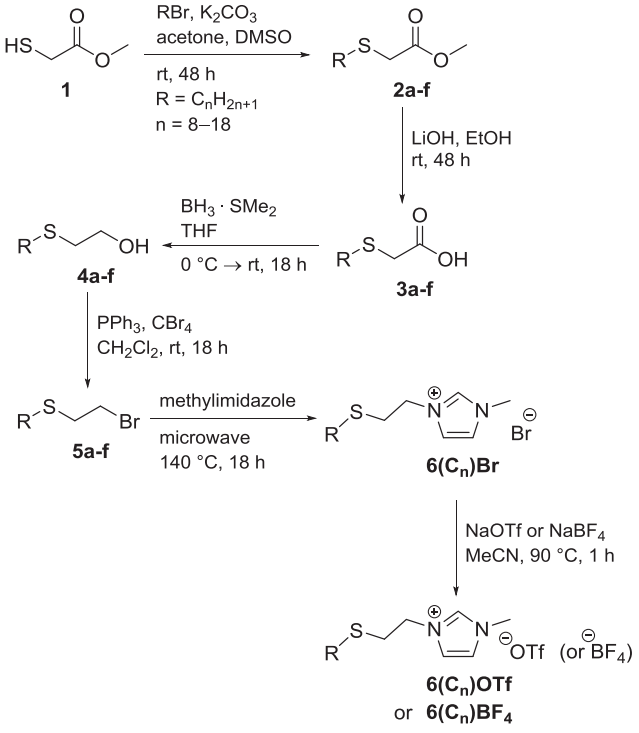

compound		yields [%]						
n	2-5	2	3	4	5	6(C_n)Br	6(C_n)OTf	6(C_n)Bf_4
8	a	96	83	80	46	56	57	-
10	b	86	83	83	30	56	91	-
12	c	92	87	96	61	59	98	-
14	d	91	quant.	95	47	62	61	-
16	e	76	92	62	45	67	87	-
18	f	quant.	95	quant.	71	91	87	87

Scheme 1. Synthesis of thioether-imidazolium ILCs **6(C_n)X**.

Table 1
Phase transition temperatures [°C] and enthalpies [kJ mol^{-1}] of thioether-imidazolium ILCs **6(C_n)X** (X=Br, OTf, BF_4)[a,b]

Entry	n	X						Heating cycle
(1)	8	Br	Cr	22 (24.0)	SmA	51 (0.2)	I	Second heat
(2)	10	Br	Cr	35 (30.2)	SmA	148 (0.7)	I	Second heat
(3)	12	Br	Cr	46	SmA	~200	I (dec)	Second heat[c]
(4)	14	Br	Cr	55	SmA	~200	I (dec)	Second heat[c]
(5)	16	Br	Cr	62	SmA	~200	I (dec)	Second heat[c]
(6)	18	Br	Cr	41	SmA	~200	I (dec)	Second heat[c]
(7)	8	OTf	Liquid					Second heat
(8)	10	OTf	Cr	4 (17.3)	I			Second heat
(9)	12	OTf	Cr	6 (11.4)	SmA	36 (0.3)	I	Second heat
(10)	14	OTf	Cr	28 (16.6)	SmA	71 (0.8)	I	Second heat
(11)	16	OTf	Cr	43 (22.4)	SmA	124 (0.7)	I	Second heat
(12)	18	OTf	Cr	54 (24.9)	SmA	149 (0.7)	I	Second heat
(13)	18	BF_4	Cr	64 (27.9)	SmA	~200	I (dec)	Second heat[c]

[a] Phase transitions were determined by DSC upon second heating. Heating/cooling rate 10 K min^{-1}.
[b] he following phases were observed: crystalline (Cr), smectic A (SmA), isotropic (I).
[c] In case of entries (3)–(6), (13) exothermal decomposition was observed during isotropization. Therefore, melting points were determined by polarizing optical microscopy (POM).

As shown in Table 1, this strategy was successful for the derivatives with the chain lengths C_{12}–C_{18}. Whereas imidazolium triflates **6(C_8)OTf** and **6(C_{10})OTf** displayed only isotropic melting (entries 7, 8), all other derivatives **6(C_n)OTf** where n=12–18 showed enantiotropic mesomorphism with almost no hysteresis (entries 9–12) (Fig. 1d). The TGA experiments further revealed that the clearing point, which is hardly visible in the DSC curve, was significantly shifted below the decomposition temperature. Replacement of the triflate counterion by tetrafluoroborate for the C_{18} derivative **6(C_{18})BF_4** showed again a pronounced tendency for decomposition during the clearing process (entry 13).

Investigations by polarizing optical microscopy (POM) yielded homeotropic textures typical for SmA phases. Characteristic examples of the obtained POM textures are shown in Fig. 2.

Upon comparison with the simple *N*-alkyl-*N*-methyl-imidazolium salts **7(C_n)X**[17] and previously-prepared amine and amide derivatives **8(C_n)X** and **9(C_{n-1})X**, respectively (Scheme 2, Fig. 3), it is clearly visible that sulfur does indeed have a beneficial effect on both the mesophase width and stability as long as triflates are concerned. Thus clearing points are increased while melting points are in the range from ambient temperature up to 55 °C. Furthermore, the clearing points of the triflates are still far below their decomposition temperatures (see Supplementary data, Fig. S1).

Small- and wide-angle X-ray diffraction measurements (SAXS and WAXS, respectively) confirmed the proposed SmA phase geometry. A representative WAXS pattern of **6(C_{18})OTf** is shown in Fig. 4 with a strong fundamental diffraction peak (001) in the small-angle region and a diffuse halo in the wide-angle region from the molten alkyl chains.

Layer spacings d_{001} were obtained at different temperatures using a Gaussian distribution on the corresponding diffraction signal (001). All thioether-linked triflates **6(C_n)OTf** showed, as seen with the previous published amines and amides,[13] a linear temperature-dependency of the layer spacing (Fig. 5), whereby the layer spacing decreased with increasing temperature. These values indicate a bilayer structure of the molecules with strongly interdigitated alkyl chains and d_{001} values of $L_{calcd}<d_{001}<2L_{calcd}$, where L_{calcd} is the length of the fully extended molecule with an all-*trans* configuration of the alkyl moiety. Layer spacings d_{red} at a reduced temperature (d_{001} at 0.95 T_{iso})[19] were determined for better comparison of the imidazolium salts bearing different groups (Table 2). For example, the calculated molecular length of **6(C_{16})OTf** is 2770 pm,[18] whereas d_{red} is 3498 pm. This concludes that the mesogens are organized in a bilayer structure (Fig. 6). The calculated layer spacing d_{calcd} is 3480 pm[18] (fully interdigitated alkyl chains of the cations 2060 pm plus two times the methyl-imidazolium core with 710 pm each), which is close to the d_{red} value of 3480 pm (Table 2). Overall, the layer spacings d_{001} increase with increasing alkyl chain length.

A comparison of the smectic layer distances d_{red} of thioethers **6(C_n)OTf** with the distances for amines **8(C_n)OTf** and amides **9(C_{n-1})OTf**, respectively, showed that the interdigitation of thioethers **6(C_n)X** lies in between smaller d_{red} values for amines **8(C_n)X** and larger d_{red} values for amides **9(C_{n-1})X** (Fig. 5).

3. Conclusion

We have presented the synthesis of novel imidazolium ionic liquid crystals bearing a thioether unit. Simple reaction conditions were used with good to quantitative yields throughout. The sulfur-linked bromides displayed decreased mesophase ranges compared to the corresponding alkylated species. After an anion exchange from Br to OTf the thioether compounds showed the widest mesophases compared to previously described amines and amides. The following trend was observed: The softer the anion, the wider was the mesophase range. All mesogens displayed smectic A mesophase geometries and with increasing alkyl chain lengths an increase of the mesophase width was observed.

XRD experiments showed an almost linear dependency of the layer spacings d_{001} with increasing temperature and a bilayer alignment of the mesogens. A maximum degree of interdigitation up to the heteroatom group is assumed for the analyzed thioethers.

Please cite this article in press as: Mansueto, M.; et al., Tetrahedron (2014), http://dx.doi.org/10.1016/j.tet.2014.03.050

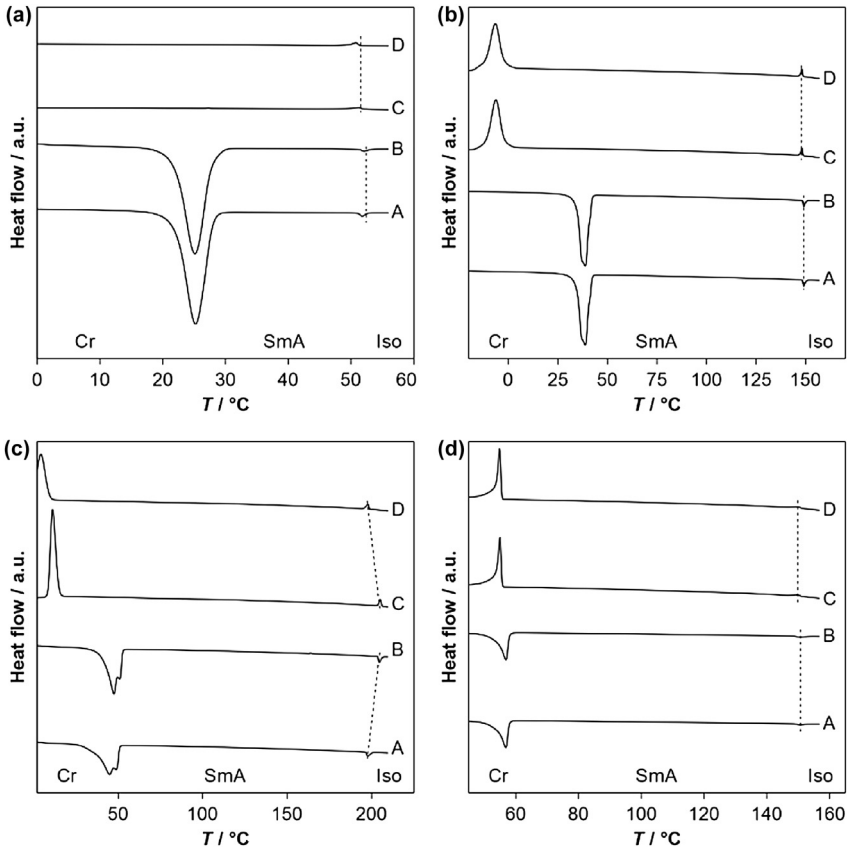

Fig. 1. DSC traces of (a) **6(C_8)Br**, (b) **6(C_{10})Br**, (c) **6(C_{12})Br** and (d) **6(C_{18})OTf** (heating/cooling rate 10 K min^{-1}). A: second heating, B: first heating, C: first cooling, D: second cooling.

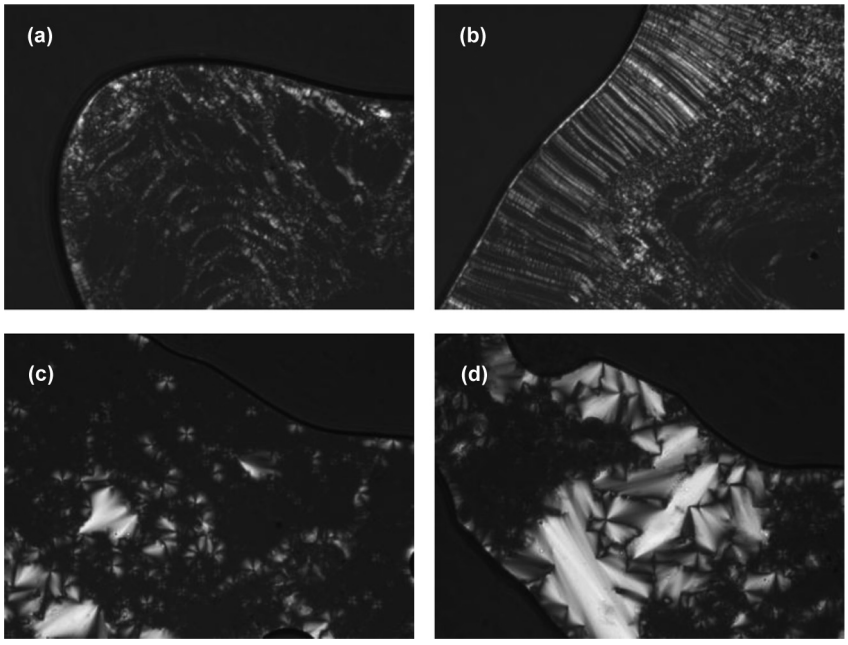

Fig. 2. Typical POM textures of thioether-linked ILCs. (a) **6(C_{12})OTf** at 10 °C (first heating), (b) **6(C_{12})OTf** at 22 °C (first heating), (c) and (d) **6(C_{18})OTf** at 126 °C (first cooling). Focal conic and Maltese cross textures indicative for a SmA mesophase. (magnification: 200×, heating/cooling rate 10 K min^{-1}).

Therefore the interdigitation of the alkyl chains decreased while increasing the linking unit.

The current work provides further insight in the structure-property relationship of imidazolium salts. The observation that mesomorphic properties of imidazolium ILCs were improved by the sulfur linker might be taken as indication that the performance of DSSCs can be further improved by such thioether ILCs as compared to *N*-methyl-*N*-alkyl-imidazolium ILCs. Those turned already out to be auspicious due to their high ionic conductivity and good pore filling property.[9,20]

Please cite this article in press as: Mansueto, M.; et al., Tetrahedron (2014), http://dx.doi.org/10.1016/j.tet.2014.03.050

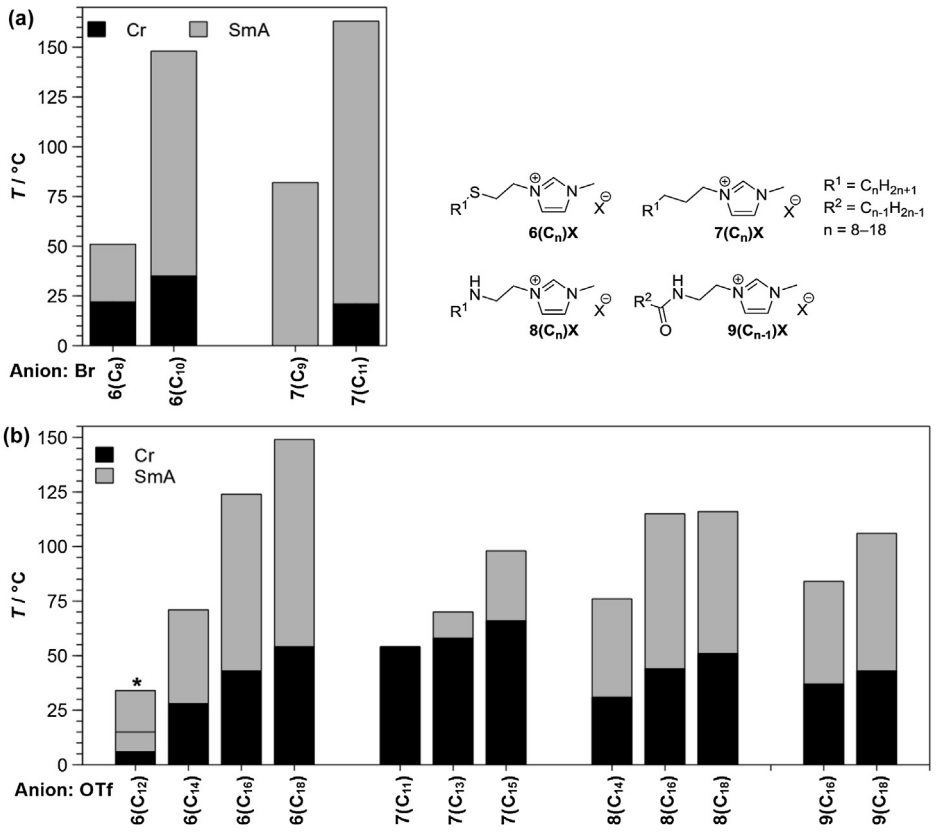

Fig. 3. Mesophase stabilities of the imidazolium derivatives with (a) bromide and (b) triflate anion. * Monotropic phase behaviour was observed. The values for amines **8(C_n)OTf** and amides **9(C_{n-1})OTf** are from Ref. 13, for **7(C_n)OTf** from Ref. 17.

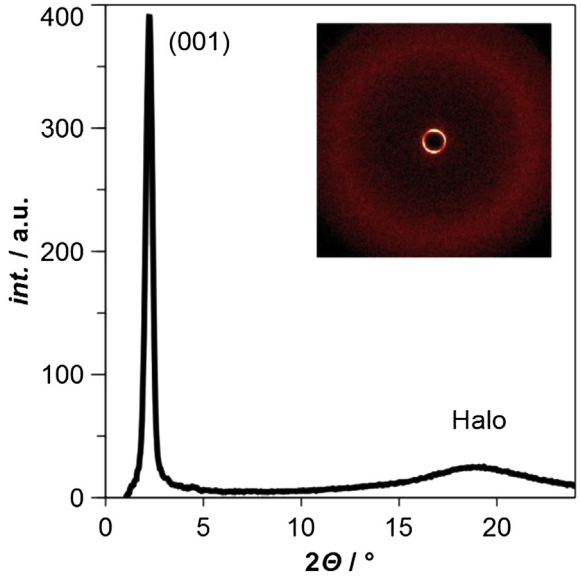

Fig. 4. Diffraction pattern of **6(C_{18})OTf** at 79 °C with the corresponding WAXS image (inset).

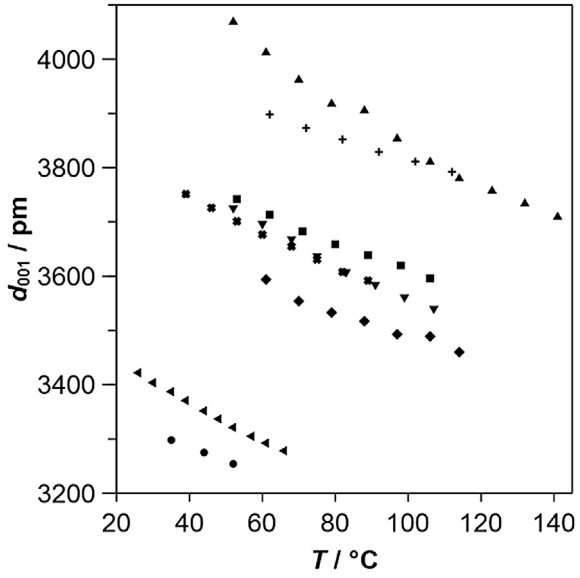

Fig. 5. Temperature dependency of the d_{001} layer spacings obtained from SAXS investigations. Key: ◂ **6(C_{14})OTf**, ▼ **6(C_{16})OTf**, ▲ **6(C_{18})OTf**, ● **8(C_{14})OTf**, ◆ **8(C_{16})OTf**, ■ **8(C_{18})OTf**, × **9(C_{16})OTf**, + **9(C_{18})OTf**. The values for amines **8(C_n)OTf** and amides **9(C_{n-1})OTf** were taken from Ref. 13.

4. Experimental section

4.1. General methods

Commercially obtained chemicals were used as received. For a better clarity and simplicity a non-IUPAC nomenclature was used. Column chromatography was carried out on silica 60Dm (40–70 mm). For thin layer chromatography silica gel sheets TLC silica gel 60 F_{254} from Merck were used. ^{1}H and ^{13}C NMR were recorded with Bruker Avance 300 and Avance 500 spectrometers at 296 K. FTIR spectra were recorded with a Bruker Vektor22 spectrometer with an MKII Golden Gate Single Reflection Diamant ATR

Please cite this article in press as: Mansueto, M.; et al., Tetrahedron (2014), http://dx.doi.org/10.1016/j.tet.2014.03.050

Table 2
Comparison of the calculated[18] and experimental layer spacings d_{red} of the imidazolium compounds **9(AA,C_n)** and **10(Gly,C_m)OTf**

Compound	T_{red}/°C	d_{red}/pm	d_{calcd}/pm
6(C_{14})OTf	68	3267	3220
6(C_{16})OTf	118	3498	3480
6(C_{18})OTf	142	3683	3730
8(C_{14})OTf	72	3205	3000
8(C_{16})OTf	109	3468	3250
8(C_{18})OTf	110	3582	3510
9(C_{16})OTf	83	3616	3600
9(C_{18})OTf	107	3783	3860

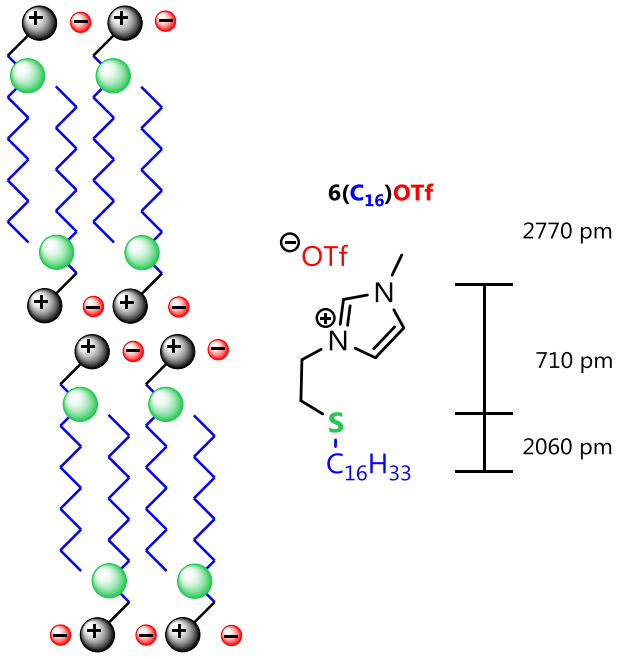

Fig. 6. Proposed packing model of the smectic phase (left) and example of the calculated layer spacing d_{calcd} of **6(C_{18})OTf** (right).

system. Mass spectrometry was performed on a Varian MAT 711 mass spectrometer with EI ionization (70 eV) and a Bruker micrOTOF_Q with electrospray ionization. Elementary analysis were performed on a Carlo Erba Strumentazione Elemental Analyzer Model 1106. Differential scanning calorimetry was performed using a Mettler Toledo DSC822 with a heating/cooling rate of 10 K min^{-1} (±1 K), melting points (uncorrected) and mesophase textures were obtained by polarizing optical microscopy using an Olympus BX 50 polarizing microscope combined with a Linkam LTS 350 hot stage. X-ray powder experiments were performed using a Bruker Nanostar with monochromatic Cu $K_{\alpha 1}$ beam (λ=1.5405 Å) was obtained using a ceramic tube generator (1500 W) with cross-coupled Göbel mirrors as the monochromator. Calibration of the patterns was carried out with the powder pattern of Ag-Behenate. Samples were prepared using glass tubes (0.7 mm outside diameter) from Fa. Hilgenberg GmbH and tempered on a temperature-controlled hot stage (±1 K).

4.2. General procedure for the synthesis of thioethers 2a–f

To a suspension of K_2CO_3 (2.80 g, 28.3 mmol) in acetone (30 mL) and DMSO (10 mL) was added successively the corresponding bromoalkane (9.42 mmol) and 2-methylmercaptoacetate **1** (1 g, 9.42 mmol). The reaction mixture was stirred for 48 h at room temperature, filtered through a Celite and the solvent was removed under reduced pressure. Solid products were poured on ice water, filtered, solubilized in CH_2Cl_2 and dried over anhydrous $MgSO_4$. Liquid products were washed with water and CH_2Cl_2 were added to the organic phase, which was dried over anhydrous $MgSO_4$. The solvent was removed in vacuum to yield the thioethers **2a–f**.[14]

*4.2.1. Methyl 2-(octadecylthio)acetate **2f**.* Colourless solid (3.40 g, 9.49 mmol, quant.). ^{1}H NMR (300 MHz, $CDCl_3$, TMS): δ=0.88 (t, J=6.8 Hz, 3H, CH_3), 1.21–1.42 (m, 30H, CH_2), 1.53–1.66 (m, 2H, SCH_2CH_2), 2.59–2.67 (m, 2H, SCH_2), 3.23 (s, 2H, $COCH_2S$), 3.74 (s, 3H, CO_2CH_3) ppm; ^{13}C NMR (75 MHz, $CDCl_3$, TMS): δ=14.1 (CH_3), 28.76, 28.98, 29.19, 29.37, 29.51, 29.59, 29.70, 31.9 (CH_2), 32.8, 33.5 (CH_2), 52.4 (CO_2CH_3), 171.1 (CO) ppm; FTIR (ATR): $\tilde{\nu}$=2916 (vs), 2849 (s), 1737 (m), 1467 (w), 1436 (w), 1280 (m), 1135 (w), 1010 (w), 721 (w) cm^{-1}; MS (ESI): m/z: 381 [MNa^+], 300 [$MNa^+-C_2H_2O_2$]; HRMS (ESI): m/z calculated for $C_{21}H_{42}NaO_2S^+$: 381.2798 [MNa^+]; found: 381.2817; mp: 34 °C.

4.3. General procedure for the deprotection to the acids 3a–f

The corresponding thioether **2a–f** (7.82 mmol) was dissolved in ethanol (300 mL) and LiOH (0.79 g, 33.0 mmol) was added and stirred for 48 h at room temperature. The reaction mixture was acidified with 1 N HCl until reaching pH=3. For solid products the mixture was poured on ice water, the solid was filtered, in CH_2Cl_2 solubilized and dried over anhydrous $MgSO_4$. For liquid products the solvent was removed in vacuo and H_2O was added. The phases were separated and the organic was dried over anhydrous $MgSO_4$. After removal of the solvent under reduced pressure **3a–f** was obtained.

*4.3.1. 2-(Octadecylthio)acetic acid **3f**.* Colourless solid (2.69 g, 7.82 mmol, 95%). ^{1}H NMR (300 MHz, $CDCl_3$, TMS): δ=0.88 (t, J=6.8 Hz, 3H, CH_3), 1.20–1.44 (m, 30H, CH_2), 1.55–1.67 (m, 2H, SCH_2CH_2), 2.61–2.70 (m, 2H, SCH_2), 3.26 (s, 2H, $COCH_2S$) ppm; ^{13}C NMR (75 MHz, $CDCl_3$, TMS): δ=14.1 (CH_3), 22.7, 28.74, 28.90, 29.19, 29.37, 29.50, 29.60, 29.67, 29.71, 31.9 (CH_2), 32.8, 33.5 (CH_2), 175.7 (CO) ppm; FTIR (ATR): $\tilde{\nu}$=2955 (w), 2916 (vs), 2874 (s), 1722 (w), 1694 (m), 1470 (w), 1460 (w), 1425 (w), 1397 (w), 1316 (w), 1267 (w), 1208 (w), 1145 (w), 1080 (w), 1031 (w), 906 (vs), 733 (vs), 650 (w) cm^{-1}; MS (ESI): m/z: 367 [MNa^+], 301 [MH^+-CO_2]; HRMS (ESI): m/z calculated for $C_{20}H_{40}NaO_2S^+$: 367.2641 [MNa^+]; found: 367.2616; mp: 84 °C.

4.4. General procedure for the preparation of alcohols 4a–f

The corresponding acid **3a–f** (0.29 mmol) was dissolved in abs. THF (10 mL), cooled to 0 °C and a borane dimethylsulfide complex solution (0.07 g, 0.09 mL, 0.87 mmol; 94% in dimethylsulfide) was added dropwise. The reaction mixture was stirred for 2 h at 0 °C and a borane dimethylsulfide complex solution (0.07 g, 0.09 mL, 0.87 mmol; 94%) was added again and the solution was allowed to reach room temperature overnight. H_2O was added slowly until the development of gas ceased. The organic solvent was removed under reduced pressure and $CHCl_3$ (10 mL) was added. The organic phase was dried over anhydrous $MgSO_4$ and the solvent was removed in vacuum yielding **4a–f**.

*4.4.1. 2-(Octadecylthio)ethanol **4f**.* Colourless solid (0.10 g, 0.30 mmol, quant.). ^{1}H NMR (300 MHz, $CDCl_3$, TMS): δ=0.88 (t, J=6.7 Hz, 3H, CH_3), 1.20–1.42 (m, 30H, CH_2), 1.52–1.64 (m, 2H, SCH_2CH_2), 2.11–2.23 (br, 1H, OH), 2.48–2.56 (m, 2H, SCH_2), 2.70–2.77 (m, 2H, SCH_2CH_2O), 3.68–3.76 (m, 2H, CH_2OH) ppm; ^{13}C NMR (75 MHz, $CDCl_3$, TMS): δ=14.1 (CH_3), 22.7, 28.87, 29.23, 29.37, 29.52, 29.60, 29.67, 29.68, 29.70, 31.59, 31.93, 33.4 (CH_2), 60.1 (CH_2OH) ppm; FTIR (ATR): $\tilde{\nu}$=2924 (m), 2853 (m), 2361 (w), 2252

(w), 1712 (w), 1466 (w), 1366 (w), 1171 (w), 1058 (w), 905 (s), 728 (vs), 649 (m) cm^{-1}; MS(EI): *m/z* (%): 330 (21) [M^+], 299 (12) [M^+-CH_3O], 285 (100) [$M^+-C_2H_5O$], 97 (6), 83 (7), 57 (8), 43 (5); HRMS (ESI): *m/z* calculated for $C_{20}H_{42}OS^+$: 330.2956 [M^+]; found: 330.2958.

4.5. General procedure for the synthesis of bromides 5a–f

The corresponding alcohol **4a–f** (0.91 mmol) and PPh_3 (0.32 g, 1.23 mmol) were dissolved in abs. CH_2Cl_2 (10 mL) and CBr_4 (0.41 g, 1.23 mmol) was added. The reaction mixture was stirred overnight at room temperature. The solvent was removed under reduced pressure and the crude product was purified through column chromatography (hexanes/EtOAc 40:1; R_f=0.7) to yield **5a–f**.[15]

*4.5.1. (2-Bromoethyl)(octadecyl)sulfane **5f**.* Colourless solid (0.25 g, 0.65 mmol, 71%). ^1H NMR (300 MHz, $CDCl_3$, TMS): δ=0.88 (t, *J*=6.8 Hz, 3H, CH_3), 1.20–1.42 (m, 30H, CH_2), 1.52–1.65 (m, 2H, SCH_2CH_2), 2.51–2.59 (m, 2H, SCH_2), 2.89–2.99 (m, 2H, SCH_2CH_2Br), 3.44–3.52 (m, 2H, CH_2Br) ppm; ^{13}C NMR (75 MHz, $CDCl_3$, TMS): δ=14.1 (CH_3), 22.7, 28.8, 29.20, 29.37, 29.51, 29.59, 29.65, 29.67, 29.71, 29.79, 30.6, 31.9 (CH_2), 32.4 (CH_2), 34.2 (CH_2Br) ppm; FTIR (ATR): $\tilde{\nu}$=2921 (vs), 2951 (s), 2360 (w), 1739 (w), 1466 (w), 1189 (w), 721 (w), 613 (w) cm^{-1}; MS(EI): *m/z* (%): 392 (7) [M^+], 313 (26), 286 (18), 285 (100), 97 (5), 69 (7), 57 (9), 43 (9); HRMS (EI): *m/z* calculated for $C_{20}H_{41}BrS^+$: 392.2112 [M^+]; found: 392.2112.

4.6. General procedure for preparation of imidazolium bromides 6(C_n)Br

The corresponding bromide **5a–f** (0.15 mmol) and 1-methylimidazole (0.12 μL, 12 mg, 0.15 mmol) were given in a microwave vial and irradiated in a microwave for 8 h at 140 °C. The crude product was recrystallized from EtOAc to afford the imidazolium bromides **6(C_n)Br**.

*4.6.1. 1-Methyl-3-(2-(octadecylthio)ethyl)-1H-imidazol-3-ium bromide **6(C_{18})Br**.* Colourless solid (64 mg, 0.13 mmol, 91%). ^1H NMR (300 MHz, $CDCl_3$, TMS): δ=0.88 (t, *J*=6.7 Hz, 3H, CH_3), 1.21–1.41 (m, 30H, CH_2), 1.51–1.63 (m, 2H, SCH_2CH_2), 2.55–2.64 (m, 2H, SCH_2), 3.01–3.09 (m, 2H, SCH_2CH_2Im), 4.09 (s, 3H, $ImCH_3$), 4.59–4.66 (m, 2H, CH_2Im), 7.22–7.24 (m, 1H, Im), 7.41–7.43 (m, 1H, Im), 10.74 (s, 1H, NCHN) ppm; ^{13}C NMR (75 MHz, $CDCl_3$, TMS): δ=14.1 (CH_3), 22.7, 28.7, 29.24, 29.37, 29.46, 29.53, 29.62, 29.67, 31.9 (CH_2), 32.39, 32.45 (CH_2), 36.6 ($ImCH_3$), 49.5 ($ImCH_2$), 122.43 (Im), 138.6 (NCHN) ppm; FTIR (ATR): $\tilde{\nu}$=3038 (w), 2953 (w), 2918 (vs), 2847 (s), 2360 (w), 1557 (w), 1466 (m), 1310 (w), 1217 (w), 1171 (m), 908 (w), 760 (w), 736 (m), 722 (m), 641 (w), 621 (w) cm^{-1}; MS (ESI): *m/z*: 395 [M^+], 313 [$M^+-C_4H_6N_2$]; HRMS (ESI): *m/z* calculated for $C_{24}H_{47}N_2S^+$: 395.2454 [M^+]; found: 395.3469; mp: 41 °C; decomposition upon reaching the clearing temperature.

4.7. General procedure for the anion exchange

The respective imidazolium bromide **6(C_n)Br** (0.13) was dissolved in MeCN (10 mL), the corresponding potassium salt (0.14 mmol) was added and stirred under reflux for 1 h. After cooling to room temperature the solvent was removed under reduced pressure, the residue dissolved in CH_2Cl_2 (10 mL) and filtered. The solvent was removed under reduced pressure to obtain the corresponding imidazolium triflates **6(C_n)OTf** or tetrafluoroborate **6(C_{18})BF_4**.

*4.7.1. 1-Methyl-3-(2-(octadecylthio)ethyl)-1H-imidazol-3-ium triflate **6(C_{18})OTf**.* Colourless solid (13 mg, 0.02 mmol, 87%). ^1H NMR (500 MHz, $CDCl_3$, TMS): δ=0.88 (t, *J*=6.9 Hz, 3H, CH_3), 1.21–1.41 (m, 30H, CH_2), 1.51–1.62 (m, 2H, SCH_2CH_2), 2.52–2.60 (m, 2H, SCH_2), 2.94–3.03 (m, 2H, SCH_2CH_2Im), 4.01 (s, 3H, $ImCH_3$), 4.41–4.49 (m, 2H, CH_2Im), 7.23–7.25 (m, 1H, Im), 7.37–7.39 (m, 1H, Im), 9.42–9.44 (m, 1H, NCHN) ppm; ^{13}C NMR (125 MHz, $CDCl_3$, TMS): δ=14.1 (CH_3), 22.7, 28.7, 29.22, 29.37, 29.43, 29.53, 29.62, 29.67, 29.71, 31.9 (CH_2), 32.15, 32.19 (CH_2), 36.6 ($ImCH_3$), 49.4 ($ImCH_2$), 122.49, 122.80 (Im), 137.9 (NCHN) ppm; FTIR (ATR): $\tilde{\nu}$=3152 (w), 3115 (w), 2957 (w), 2918 (vs), 2850 (s), 2361 (w), 2253 (w), 1667 (w), 1576 (W), 1468 (w), 1379 (w), 1337 (w), 1256 (vs), 1225 (m), 1162 (s), 1031 (s), 908 (m), 735 (s), 639 (s), 621 (w), 574 (w) cm^{-1}; MS (ESI): *m/z*: 395 [M^+], 335, 313 [$M^+-C_4H_6N_2$]; 149 [M^-]; HRMS (ESI): *m/z* calculated for $C_{24}H_{47}N_2S^+$: 395.3454 [M^+]; found: 395.3434; calculated for $CF_3O_3S^-$: 148.9515 [M^-]; found: 148.9534; DSC: Cr 54 °C [24.9 kJ mol^{-1}] SmA 149 °C [0.7 kJ mol^{-1}] I.

*4.7.2. 1-Methyl-3-(2-(octadecylthio)ethyl)-1H-imidazol-3-ium tetrafluoroborate **6(C_{18})BF_4**.* Colourless solid (13 mg, 0.02 mmol, 87%). ^1H NMR (500 MHz, $CDCl_3$, TMS): δ=0.88 (t, *J*=6.9 Hz, 3H, CH_3), 1.18–1.41 (m, 30H, CH_2), 1.52–1.62 (m, 2H, SCH_2CH_2), 2.53–2.62 (m, 2H, SCH_2), 2.95–3.05 (m, 2H, SCH_2CH_2Im), 4.02 (s, 3H, $ImCH_3$), 4.45–4.53 (m, 2H, CH_2Im), 7.22–7.25 (m, 1H, Im), 7.38–7.41 (m, 1H, Im), 9.64–9.69 (m, 1H, NCHN) ppm; ^{13}C NMR (125 MHz, $CDCl_3$, TMS): δ=14.1 (CH_3), 22.7, 28.8, 29.24, 29.37, 29.45, 29.54, 29.63, 29.67, 29.68, 29.71, 31.9 (CH_2), 32.23, 32.26 (CH_2), 36.7 ($ImCH_3$), 49.5 ($ImCH_2$), 122.47, 122.74 (Im), 137.8 (NCHN) ppm; FTIR (ATR): $\tilde{\nu}$=3161 (w), 2958 (w), 2923 (m), 2852 (m), 2364 (w), 1575 (w), 1467 (w), 1379 (w), 1261 (w), 1171 (w), 1057 (m), 907 (s), 731 (vs), 646 (w), 622 (w) cm^{-1}; MS (ESI): *m/z*: 395 [M^+], 335, 313 [$M^+-C_4H_6N_2$]; 87 [M^-]; HRMS (ESI): *m/z* calculated for $C_{24}H_{47}N_2S^+$: 395.3454 [M^+]; found: 395.3434; calculated for BF_4^-: 87.0024 [M^-]; found: 87.0027; DSC: Cr 64 °C [27.9 kJ mol^{-1}]; decomposition upon reaching the clearing temperature.

Acknowledgements

Generous financial support by the Ministerium für Wissenschaft, Forschung und Kunst des Landes Baden-Württemberg, the Bundesministerium für Bildung und Forschung (shared instrumentation grant #01 RI 05177) and the Fonds der Chemischen Industrie is gratefully acknowledged. We would like to thank Christoph Schneck for the TGA experiments.

Supplementary data

Further experimental results and supplementary figures. Supplementary data related to this article can be found at http://dx.doi.org/10.1016/j.tet.2014.03.050.

References and notes

1. Reviews: (a) Colella, N. S.; Zhang, L.; Briseno, A. L. *Mater. Matters* **2012**, *7*, 18–20; (b) Bunz, U. H. *Angew. Chem., Int. Ed.* **2010**, *49*, 5037–5040; (c) *Handbook of Thiophene-Based Materials*; Perepichka, I. F., Perepichka, D. F., Eds.; 2009; vol. 2, pp 595–646; (d) Mishra, A.; Ma, C.-Q.; Bäuerle, P. *Chem. Rev.* **2009**, *109*, 1141–1276; (e) Torroba, T.; García-Valverde, M. *Angew. Chem., Int. Ed.* **2006**, *45*, 8092–8096.
2. Reviews: (a) Martín, N. *Chem. Commun.* **2013**, 7025–7027; (b) Zhao, Y.; Chen, G.; Mulla, K.; Mahmud, I.; Liang, S.; Dongare, P.; Thompson, D. W.; Dawe, L. N.; Bouzan, S. *Pure Appl. Chem.* **2012**, *84*, 1005–1025; (c) Salle, M.; Canevet, D.; Balandier, J.-Y.; Lyskawa, J.; Trippe, G.; Goeb, S.; Le Derf, F. *Phosphorus, Sulfur Silicon Relat. Elem.* **2011**, *186*, 1153–1168; (d) Nielsen, M. B. *Phosphorus, Sulfur Silicon Relat. Elem.* **2011**, *186*, 1055–1073; (e) Canevet, D.; Sallé, M.; Zhang, G.; Zhang, D.; Zhu, D. *Chem. Commun.* **2009**, 2245–2269; (f) Herranz, M. Á.; Sánchez, L.; Martín, N. *Phosphorus, Sulfur Silicon Relat. Elem.* **2005**, *180*, 1133–1148.
3. Reviews: (a) Seed, A. *Chem. Soc. Rev.* **2007**, *36*, 2046–2069; (b) Bryce, M. R. *J. Mater. Chem.* **2000**, *10*, 589–598.
4. Recent examples: (a) Folcia, C. L.; Ortega, J.; Etxebarria, J.; Rodríguez-Conde, S.; Sanz-Enguita, G.; Geese, K.; Tschierske, C.; Ponsinet, V.; Barois, P.; Pindak, R.; Pan, L.; Liu, Z. Q.; McCoy, B. K.; Huang, C. C. *Soft Matter* **2013**, *10*, 196–205; (b) Cheng, W.-C.; Yang, C.-Y.; Kang, B.-Y.; Kuo, M.-Y.; Ruan, J. *Soft Matter* **2013**, *9*,

10822–10831; (c) Reddy, M. K.; Reddy, K. S.; Prakash, M.; Narasimhaswamy, T. *Mol. Cryst. Liq. Cryst.* **2013**, *582*, 1–14; (d) Dong, J.; Kawabata, K.; Seino, T.; Yang, F.; Goto, H. *Liq. Cryst.* **2013**, *40*, 1455–1465; (e) Chen, X.; Chen, L.; Yao, K.; Chen, Y. *ACS Appl. Mater. Interfaces* **2013**, *5*, 8321–8328; (f) Cheng, X.; Gao, H.; Tan, X.; Yang, X.; Prehm, M.; Ebert, H.; Tschierske, C. *Chem. Sci.* **2013**, *4*, 3317–3331; (g) Hegde, G.; Alla, R. A.; Matharu, A.; Komitov, L. *J. Mater. Chem. C* **2013**, *1*, 3600–3605; (h) Bu, W.; Gao, H.; Tan, X.; Dong, X.; Cheng, X.; Prehm, M.; Tschierske, C. *Chem. Commun.* **2013**, 1756–1758; (i) Yin, B.; Zhong, K.; Jiang, S.; Wang, H.; Hou, R. *Heterocycles* **2012**, *85*, 3021–3028; (j) Garcia, G.; Moral, M.; Granedino-Roldán, J. M.; Garzón, A.; Navarro, A.; Fernández-Gomez, M. *J. Phys. Chem. C* **2013**, *117*, 15–22.

5. Sergeyev, S.; Pisula, W.; Geerts, Y. H. *Chem. Soc. Rev.* **2007**, *36*, 1902–1929.
6. (a) Savage, R. C.; Mativetsky, J. M.; Orgiu, E.; Palma, M.; Gbabode, G.; Geerts, Y. H.; Samorí, P. *J. Mater. Chem.* **2010**, *21*, 206–213; (b) Lemaur, V.; da Silva Filho, D. A.; Coropceau, V.; Lehmann, M.; Geerts, Y.; Piris, J.; Debije, M. G.; van de Craats, A. M.; Senthilkumar, K.; Siebbeles, L. D. A.; Warman, J. M.; Brédas, J.-L.; Cornil, J. *J. Am. Chem. Soc.* **2004**, *126*, 3271–3279; (c) Cornil, J.; Lemaur, V.; Calbert, J.-P.; Brédas, J.-L. *Adv. Mater.* **2002**, *14*, 726–729; (d) Adam, D.; Schuhmacher, P.; Simmerer, J.; Häussling, L.; Siemensmeyer, K.; Etzbachi, K. H.; Ringsdorf, H.; Haarer, D. *Nature* **1994**, *371*, 141–143.
7. Reviews: (a) Ringstrand, B.; Kaszynski, P. *Acc. Chem. Res.* **2013**, *46*, 214–215; (b) Chen, S.; Eichhorn, S. H. *Isr. J. Chem.* **2012**, *52*, 830–843; (c) Axenov, K. V.; Laschat, S. *Materials* **2011**, *4*, 206–259; (d) Douce, L.; Suisse, J.-M.; Guillon, D.; Taubert, A. *Liq. Cryst.* **2011**, *38*, 1653–1661; (e) Kato, T.; Mizoshita, N.; Kishimoto, K. *Angew. Chem., Int. Ed.* **2006**, *45*, 38–68; (f) Binnemans, K. *Chem. Rev.* **2005**, *105*, 4148–4204.
8. Rondla, R.; Lin, J. C. Y.; Yang, C. T.; Lin, I. J. B. *Langmuir* **2013**, *29*, 11779–11785.
9. Costa, R. D.; Werner, F.; Wang, X.; Groenninger, P.; Feihl, S.; Kohler, F. T. U.; Wasserscheid, P.; Hibler, S.; Beranek, R.; Meyer, K.; Guld, D. M. *Adv. Energy Mater.* **2013**, *3*, 657–665.
10. Chi, W. S.; Jeon, H.; Kim, S. J.; Kim, D. J.; Kim, J. H. *Macromol. Res.* **2013**, *21*, 315–320.
11. Recent examples: (a) Ji, S.-P.; Tang, M.; He, L.; Tao, G.-H. *Chem.—Eur. J.* **2013**, *19*, 4452–4461; (b) Abate, A.; Petrozza, A.; Cavallo, G.; Lanzani, G.; Matteucci, F.; Bruce, D. W.; Houbenov, N.; Metrangolo, P.; Resnati, G. *J. Mater. Chem. A* **2013**, *1*, 6572–6578; (c) Rohini, R.; Lee, C.-K.; Lu, J.-T.; Lin, I. J. B. *J. Chin. Chem. Soc.* **2013**, *60*, 745–754; (d) Westphal, E.; da Silva, D. H.; Molin, F.; Gallardo, H. *RSC Adv.* **2013**, *3*, 6442–6454; (e) Yang, M.; Mallick, B.; Mudring, A.-V. *Cryst. Growth Des.* **2013**, *13*, 3068–3077; (f) Schenkel, M. R.; Shao, R.; Robertson, L. A.; Wiesenauer, B. R.; Clark, N. A.; Gin, D. L. *Liq. Cryst.* **2013**, *40*, 1067–1081; (g) Ji, Y.; Shi, R.; Wang, Y.; Saielli, G. *J. Phys. Chem. B* **2013**, *117*, 1104–1109; (h) Gao, Y.; Slattery, J. M.; Bruce, D. W. *New J. Chem.* **2011**, *35*, 2910–2918; (i) Ichikawa, T.; Yoshio, M.; Taguchi, S.; Kagimoto, J.; Ohno, H.; Kato, T. *Chem. Sci.* **2012**, *3*, 2001–2008; (j) Getsis, A.; Mudring, A.-V. *Eur. J. Inorg. Chem.* **2011**, *2011*, 3207–3213; (k) Starkulla, G.; Kaller, M.; Frey, W.; Axenov, K. V.; Laschat, S. *Liq. Cryst.* **2011**, *38*, 1515–1529; (l) Getsis, A.; Mudring, A.-V. *Z. Anorg. Allg. Chem.* **2010**, *636*, 1726–1734.
12. (a) Causin, V.; Saielli, G. *J. Mater. Chem.* **2009**, *19*, 9153–9162; (b) Yazaki, S.; Funahashi, M.; Kagimoto, J.; Ohno, H.; Kato, T. *J. Am. Chem. Soc.* **2010**, *132*, 7702–7708; (c) Yazaki, S.; Funahashi, M.; Kato, T. *J. Am. Chem. Soc.* **2008**, *130*, 13206–13207; (d) Bhowmik, P. K.; Han, H.; Cebe, J. J.; Burchett, R. A.; Acharya, B.; Kumar, S. *Liq. Cryst.* **2003**, *30*, 1433–1440; (e) Kijima, M.; Setoh, K.; Shirakawa, H. *Chem. Lett.* **2000**, *29*, 936–937; (f) Haramoto, Y.; Yin, M.; Matukawa, Y.; Ujiie, S.; Nanasawa, M. *Liq. Cryst.* **1995**, *19*, 319–320.
13. Mansueto, M.; Frey, W.; Laschat, S. *Chem.—Eur. J.* **2013**, *19*, 16058–16065.
14. Jones, P. B.; Prrish, N. M.; Houston, T. A.; Stapon, A.; Bansal, N. P.; Dick, J. D.; Townsend, C. A. *J. Med. Chem.* **2000**, *43*, 3304–3314.
15. Kukovinets, O. S.; Kukovinets, A. G.; Kasradze, V. G.; Salimova, E. V.; Abdullin, M. I. *Russ. J. Org. Chem.* **2010**, *46*, 798–806.
16. Butschies, M.; Haenle, J. C.; Tussetschläger, S.; Laschat, S. *Liq. Cryst.* **2013**, *40*, 52–71.
17. Bradley, A. E.; Hardacre, C.; Holbrey, J. D.; Johnston, S.; McMath, S. E. J.; Nieuwenhuyzen, M. *Chem. Mater.* **2002**, *14*, 629–635.
18. Cambridgsoft, Chem3D Pro 12, 2013.
19. Kouwer, P. H. J.; Swager, T. M. *J. Am. Chem. Soc.* **2007**, *129*, 14042–14052.
20. Wang, H.; Zhang, X.; Gong, F.; Zhou, G.; Wang, Z.-S. *Adv. Mater.* **2012**, *24*, 121–124.

Please cite this article in press as: Mansueto, M.; et al., Tetrahedron (2014), http://dx.doi.org/10.1016/j.tet.2014.03.050